journal

J. Am. Ceram. Soc., 93 [1] 176–183 (2010)
DOI: 10.1111/j.1551-2916.2009.03382.x

Oxygen Diffusivities and Surface Exchange Coefficients in Porous Mullite/Zirconia Composites Measured by the Conductivity Relaxation Method

Hong-Da Ko and Chien-Cheng Lin*,†

Department of Materials Science and Engineering, National Chiao Tung University, Hsinchu 30050, Taiwan

Oxygen diffusivities and surface exchange coefficients in various porous mullite/zirconia composites were measured at oxygen partial pressures ranging from 20.2 to 2.02 kPa using the conductivity relaxation method. However, the oxygen diffusivities in porous high-zirconia composites could not be determined because of the predominant surface exchange reaction. Oxygen diffusivities and surface exchange coefficients in low-zirconia composites increased with the zirconia content, while the surface exchange coefficients in high-zirconia composites were approximately constant. A percolation threshold of the surface exchange coefficients occured at ~40 vol% zirconia for porous zirconia/mullite composites. The oxygen diffusivities in porous low-zirconia composites were independent of the oxygen partial pressure, implying that oxygen diffusion in these composites was related to the migration of oxygen vacancies, whose concentration was independent of the oxygen partial pressure. The surface exchange coefficients of high-zirconia composites decreased with increasing oxygen partial pressure. Finally, it was inferred that the rate-limiting step for oxygen surface exchange could be the charge-transfer process.

I. Introduction

MULLITE is a frequently used material for applications at high temperatures due to its advantageous properties, including good creep resistance, excellent chemical stability, and suitable high-temperature strength.[1] In addition, mullite is a potential substrate material because it has a favorable dielectric constant and thermal expansion coefficient.[2] To further improve its mechanical properties (e.g., fracture toughness), zirconia particles and/or silicon carbide whiskers have been incorporated into mullite, as indicated in previous studies.[3–6]

One can modify the properties of composite materials by combining two or more components. The properties of composites are highly dependent on the size, shape, and content of the individual components. Previous studies[7,8] investigated the oxygen diffusivities and electrical conductivities of mullite/zirconia composites with various zirconia contents. The percolation phenomenon for oxygen diffusion in mullite/zirconia composites was observed at 30–40 vol% zirconia, while no such phenomenon was observed for electrical conduction.[8] The electrical conductivities of mullite/zirconia composites followed Lichtenecker's rule at high frequencies and the general mixing equation at low frequencies.

Recently, the mechanical properties of porous mullite/zirconia composites have been investigated.[9,10] Haslam and Lange[9] developed a processing method to strengthen porous mullite/zirconia composites without shrinkage using evaporation/condensation sintering in an HCl atmosphere. Latella and Mehrtens[10] indicated that the mullite/zirconia composites with 62% porosity showed no strength degradation at temperatures ranging from 25° to 1200°C. Because porous composites could be used in hot gas filtration environments, the influence of zirconia content on diffusion and/or the surface exchange rate in porous mullite/zirconia composites is an important subject.

To date, little research has been conducted on the nature of mass transfer in porous mullite/zirconia composites. In a previous study, Ganeshananthan and Virkar[11] measured the oxygen surface exchange coefficients of porous $La_{0.6}Sr_{0.4}CoO_{3-\delta}$ using the conductivity relaxation method. In this study, the conductivity relaxation method was used to measure the diffusivities and surface exchange coefficients of porous mullite/zirconia composites with various zirconia contents. The effects of zirconia content and oxygen partial pressure on the diffusivities and surface exchange coefficients of porous mullite/zirconia composites were explored.

II. Experimental Procedure

Based on a previous study on the percolation phenomenon, mullite/zirconia composites containing more than 40 vol% zirconia were defined as "high-zirconia composites"; otherwise, the composites were categorized as "low-zirconia composites."

The composites in this study were fabricated by sintering mixtures of mullite (KM-mullite, 71.86 wt% Al_2O_3, 28.07 wt% SiO_2, 0.03 wt% Fe_2O_3, 0.03 wt% NaO_2, and 0.01 wt% MgO_2, 0.2 μm on average, Kyoritsu Ceramic Materials Co., Nagoya, Japan), 3 mol% Y_2O_3-stabilized ZrO_2 or 3Y–ZrO_2 powder (TZ-3Y, 94.75 wt% ZrO_2, 5.21 wt% Y_2O_3, 0.005 wt% Al_2O_3, 0.005 wt% SiO_2, 0.002 wt% Fe_2O_3, and 0.022 wt% NaO_2, 0.3 μm on average, Toyo Soda Mfg., Co., Tokyo, Japan), and carbon (Vulcan XC72, 0.03 μm on average, Cabot Co., Billerica, MA), wherein 30 vol% carbon was used as the pore-forming agent.

The starting powders were first dispersed in alcohol. The pH value was adjusted to 10 using NH_4OH as an electrolyte, and then the powder mixtures were dried on a hot plate. Subsequently, they were uniaxially pressed at 63 MPa for a few minutes. The cold-pressed samples were heated to burn out carbon at 600°C for 30 min and then sintered at 1200°–1550°C for 2–3 h depending on the composition of the powder mixture.

The densities of the sintered bodies were determined by the Archimedes method using deionized water as an immersing medium, and the relative densities were then calculated. The designations, compositions, sintering conditions, and relative densities of these composites are listed in Table I. The sintered composites were cut into pieces about $3.5 \times 3.5 \times 0.8$ mm in size. Samples were ground and polished with a precision polishing machine (Model Minimet 1000, Buehler Ltd, Lake Bluff, IL) using standard procedures as described previously.[7]

The conductivity relaxation method was used to measure the electrical resistivities of bulk samples under different oxygen

J. Stevenson—contributing editor

Manuscript No. 25864. Received February 10, 2009; approved August 14, 2009.
Research supported by National Science Council of Taiwan under Contract No. NSC 96-2221-E-009-100.
*Member, American Ceramic Society.
†Author to whom correspondence should be addressed. e-mail: chienlin@cc.nctu.edu.tw

Table I. Designations, Compositions, Sintering Conditions, and Relative Densities of Various Mullite/Zirconia Composites

Designation	Composition*	Sintering conditions	Relative density (%)
M	(100 v/o M+0 v/o Z)+30 v/o C	1550°C/3 h/air	46.3
MZY05	(95 v/o M+5 v/o Z)+30 v/o C	1400°C/3 h/air	44.9
MZY10	(90 v/o M+10 v/o Z)+30 v/o C	1400°C/3 h/air	45.2
MZY20	(80 v/o M+20 v/o Z)+30 v/o C	1400°C/3 h/air	47.5
MZY30	(70 v/o M+30 v/o Z)+30 v/o C	1350°C/2 h/air	46.8
MZY40	(60 v/o M+40 v/o Z)+30 v/o C	1350°C/2 h/air	50.9
MZY50	(50 v/o M+50 v/o Z)+30 v/o C	1300°C/2 h/air	44.5
MZY60	(40 v/o M+60 v/o Z)+30 v/o C	1300°C/2 h/air	51.8
MZY80	(20 v/o M+80 v/o Z)+30 v/o C	1200°C/2 h/air	43.1
Z	(0 v/o M+100 v/o Z)+30 v/o C	1200°C/2 h/air	47.5

*M = mullite; Z = 3 mol% Y_2O_3–ZrO_2 (3Y-PSZ); C = carbon. The carbon content (30 vol%) is based on the individual powder mixtures, while the contents included in parentheses are based on the final sintered composites.

partial pressures. Figure 1 shows a schematic diagram of the conductivity-measuring system. The specimen, together with two Pt electrodes, was clipped by two plates of Al_2O_3. After being connected to an electric potentiometer, the specimen was placed in an Al_2O_3 tube furnace. The measuring temperatures were less than the sintering temperature by at least 200°C to avoid densification during the measurements. When the electric conductivity was saturated at a certain oxygen partial pressure (pO_2^1), a gas mixture with a decreased oxygen partial pressure (pO_2^2) was introduced into the chamber. While the oxygen partial pressure changed from pO_2^1 to pO_2^2, the variation of electrical resistance was recorded with a multimeter (Model 2000, Keithley Instruments Inc., Cleveland, OH). This procedure was repeated using a stepwise decrease in the oxygen partial pressure after the electric conductivity was saturated again.

It was noted that when the ratio of initial to final pO_2 was larger than 20, linear exchange kinetics were no longer valid.[12] Thus, a narrow pO_2 change was conducted to ensure that systematic error in measuring the diffusivities and surface exchange coefficients could be avoided. The oxygen partial pressures chosen in this study were 20.2, 14.1, 10.1, 6.07, and 2.02 kPa in sequence. Variation of the oxygen partial pressure was achieved by different flow rates of oxygen and argon.

III. Mathematical Background

Transport of oxygen ions in a porous sample consists of two possible rate-controlling processes in series: the surface exchange reaction at the gas/solid interface and ionic diffusion through the bulk. If the oxygen concentration at any cross-section is kept constant, i.e., the flux into the cross-section is equal to the flux out of the cross-section, a steady-state is reached. When the oxygen partial pressure is changed in a steady-state system, the variation of oxygen concentration in the solid with time can be correlated with the rates of bulk diffusion and surface exchange by the following equation:[13]

$$\frac{M_t}{M_\infty} = 1 - \sum_{n=1}^{\infty} \frac{2L^2 \exp\left(-\frac{t}{\tau_n}\right)}{\beta_n^2(\beta_n^2 + L^2 + L)} \tag{1}$$

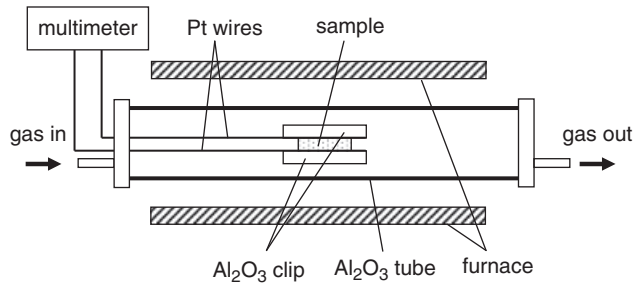

Fig. 1. Schematic diagram of the conductivity-measuring system.

where M_t is the total amount of ions that entered (or left) the sample in time t, M_∞ is the total amount of ions that entered (or left) the sample after an infinite time, τ_n is the relaxation time, and β_n are the positive roots of the following equation:

$$\beta \tan \beta = L = \frac{l\alpha}{D} \tag{2}$$

where α is the surface exchange coefficient, D is the diffusivity, and l is the half-thickness of the membrane. As a result, the relaxation time τ_n can be expressed as follows:

$$\tau_n = \frac{l^2}{D\beta_n^2} \tag{3}$$

Either bulk diffusion or surface exchange reactions can be a rate-limiting step in the relaxation process, and the ratio of diffusivity to the surface exchange coefficient is defined as the characteristic length (L_c).[14,15] When the thickness of the membrane is much larger than the characteristic length, diffusion will govern the relaxation process. In such a case, where diffusion controls ionic transport, Eq. (1) can be expressed as

$$\frac{M_t}{M_\infty} = 1 - \sum_{n=0}^{\infty} \frac{8}{(2n+1)^2\pi^2} \exp\left[\frac{-D(2n+1)^2\pi^2 t}{4l^2}\right] \tag{4}$$

In contrast, when the thickness of the membrane is much smaller than the characteristic length, the relaxation process is mainly dominated by the surface exchange reaction. In such a case, where surface exchange controls ionic transport, Eq. (1) can be simplified as

$$\frac{M_t}{M_\infty} = 1 - \exp\left(-\frac{\alpha t}{l}\right) \tag{5}$$

The equations mentioned above for the relaxation experiment are derived under the assumption of immediate change of oxygen partial pressure. When a relaxation experiment is performed in a large reactor volume or at a relatively high temperature, the time needed to change the oxygen partial pressure cannot be neglected. The relaxation time can be close to the flush time of the reactor volume, and a correction should be used. The flush time correction in a relaxation experiment was presented by den Otter *et al.*[16] Thus, Eq. (1) can be written in terms of the flush time of the reactor volume:

$$g(t) = 1 - \exp\left(-\frac{t}{\tau_f}\right) - \sum_{n=1}^{\infty} \frac{2L^2 \frac{\tau_n}{\tau_n - \tau_f}\left[\exp\left(-\frac{t}{\tau_n}\right) - \exp\left(-\frac{t}{\tau_f}\right)\right]}{\beta^2(\beta^2 + L^2 + L)} \tag{6}$$

where $g(t)$ is the normalized conductivity and τ_f is the flush time of the reactor volume or the time needed to flush the reactor volume. Since the relaxation process is controlled by surface exchange, Eq. (6) can be simplified as

$$g(t) = 1 - \exp\left(-\frac{t}{\tau_f}\right) - \frac{\tau}{\tau - \tau_f} \times \left[\exp\left(-\frac{t}{\tau}\right) - \exp\left(-\frac{t}{\tau_f}\right)\right] \quad (7)$$

where the relaxation time $\tau = l/\alpha$. Additionally, the relationship between the normalized conductivity $g(t)$ and electrical conductivities can be described by

$$g(t) = \frac{\sigma(t) - \sigma(0)}{\sigma(\infty) - \sigma(0)} = \frac{M_t}{M_\infty} \quad (8)$$

where $\sigma(0)$ is the initial conductivity and $\sigma(t)$ and $\sigma(\infty)$ are the conductivities at time t and after infinite time, respectively.

IV. Results and Discussion

(1) Conductivities

Figure 2 shows the plot of electrical resistance versus time for MZY80 at 750°C while the oxygen partial pressure was changed stepwise from 6.07 to 2.02 kPa. When the system reached an equilibrium state at 6.07 kPa, the resistance approached a certain value. Once the oxygen partial pressure was changed to 2.02 kPa, there was a dramatic increase in resistance and then another equilibrium value was approached. The normalized conductivity $g(t)$ can thus be calculated by setting $\sigma(0)$ and $\sigma(\infty)$ equal to the equilibrium conductivities at 6.07 and 2.02 kPa, respectively, while $\sigma(t)$ is the conductivity at time t after the pressure is changed.

Figure 3 displays the relationship between the conductivity and oxygen partial pressure for various composites. The conductivities of these composites increased significantly with the zirconia content and increased slightly with oxygen partial pressure. The zirconia content had a larger effect on the conductivity than the oxygen partial pressure did. The slopes of linear log conductivity versus log oxygen partial pressure curves were between 0.06 and 0.1. For *p*-type electronic conduction, the slope of a logarithmic plot of the electronic conductivity versus oxygen partial pressure was calculated to be 1/4.[17,18] The fact that the slopes obtained in this study were much lower than 1/4 suggests a significant contribution of ionic conduction.

The relation among the ionic conductivity, electron-hole conductivity, and oxygen partial pressure can be expressed by the following equation[19]:

$$\sigma_t = \sigma_i + \sigma_h^0 p O_2^{1/4} \quad (9)$$

where σ_t is the total conductivity, σ_i is the ionic conductivity, and σ_h^0 is the electron-hole conductivity at 1 atm oxygen partial pressure. Consequently, σ_i and σ_h^0 can be determined, respectively, by the intercept and slope of the total conductivity versus $pO_2^{1/4}$ curve. Table II lists the calculated ionic transport numbers $t_i = \sigma_i/(\sigma_i + \sigma_h^0)$ of mullite/zirconia composites at various temperatures, which were widely distributed between 0.12 and 0.83. This result indicates that mullite/zirconia composites are mixed ionic and electronic conducting (MIEC) materials.

Figure 4 illustrates the relationship between the normalized conductivity and time for mullite/zirconia composites at a fixed

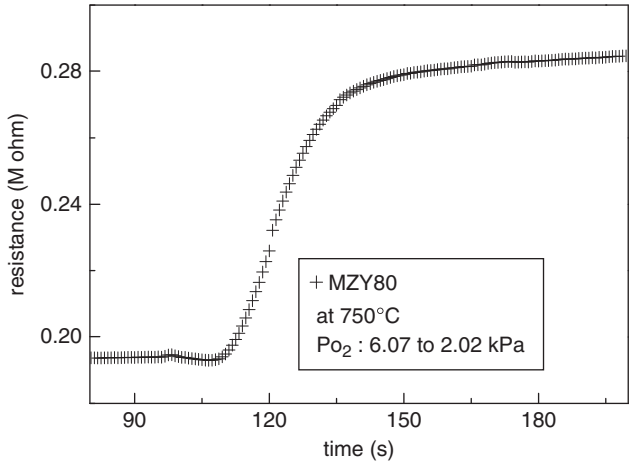

Fig. 2. Electrical resistance as a function of time for MZY80 at 750°C when the oxygen partial pressure was changed stepwise from 6.07 to 2.02 kPa.

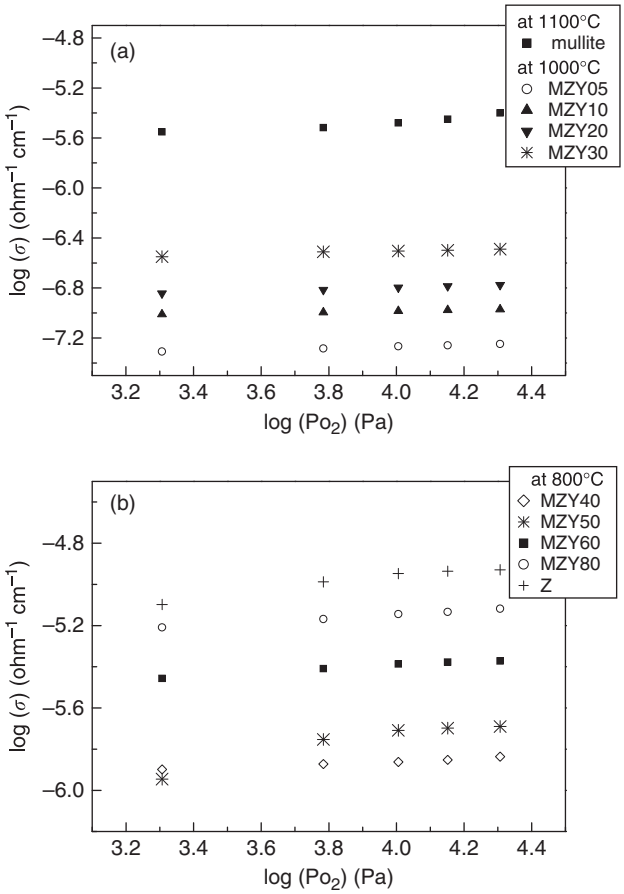

Fig. 3. Conductivity versus oxygen partial pressure curves for (a) mullite at 1100°C and low-zirconia composites at 1000°C; (b) high-zirconia composites at 800°C.

Table II. Ionic Transport Numbers of Mullite/Zirconia Composites at Various Temperatures

	Ionic transport numbers							
Composites	750°C	800°C	850°C	900°C	1000°C	1100°C	1200°C	1300°C
M	—	—	—	—	—	0.53	0.35	0.31
MZY05	—	—	—	—	0.60	0.65	0.54	—
MZY10	—	—	—	0.53	0.72	0.83	—	—
MZY20	—	—	—	0.41	0.57	0.67	—	—
MZY30	—	0.26	—	0.52	0.62	—	—	—
MZY40	0.61	0.61	0.48	—	—	—	—	—
MZY50	0.54	0.46	0.40	—	—	—	—	—
MZY60	0.17	0.20	0.12	—	—	—	—	—
MZY80	0.12	0.13	0.14	—	—	—	—	—
Z	0.68	0.48	0.41	—	—	—	—	—

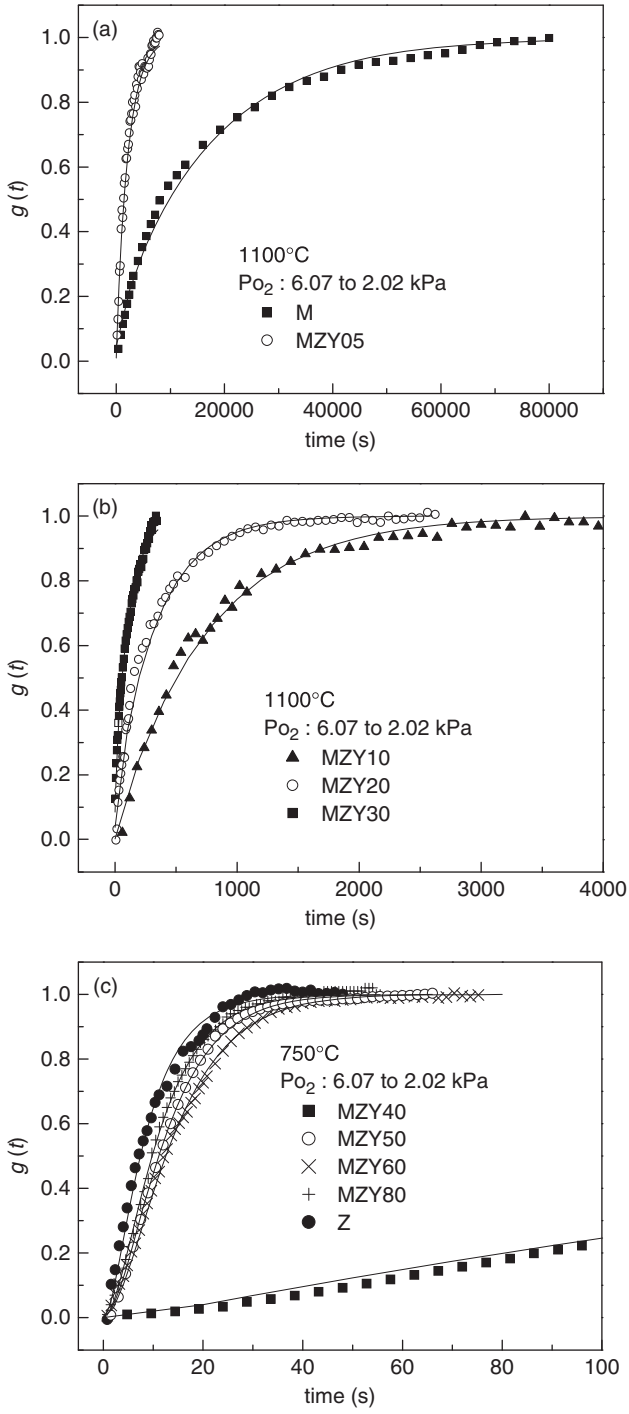

Fig. 4. Plots of the normalized conductivity $g(t)$ versus time for (a) M and MZY05 at 1100°C; (b) MZY10, MZY20, and MZY30 at 1000°C; (c) MZY40, MZY50, MZY60, MZY80, and *Z* at 750°C with the oxygen partial pressure switched from 6.07 to 2.02 kPa. The fitting lines in (a) and (b) were based on Eq. (1), and those in (c) were based on Eq. (7).

temperature with the oxygen partial pressure changed stepwise from 6.07 to 2.02 kPa. Figure 4(a) illustrates that the required time for re-equilibration in mullite at 1100°C was about 80 000 s, which was much longer than that of MZY05. Similarly, the re-equilibration time of MZY10 at 1000°C was longer than those of MZY20 and MZY30, as shown in Fig. 4(b). In other words, the re-equilibration time of low-zirconia composites decreased with increasing zirconia content. Figure 4(c), however, indicates that the re-equilibration times of high-zirconia composites at 750°C were similar, except for MZY40. When the oxygen partial pressure was changed from 6.07 to 2.02 kPa, the re-equilibration time of MZY40 at 750°C was about 700 s, which was about one order of magnitude larger than those of MZY50, MZY60, MZY80, and *Z*.

(2) Diffusivities and Surface Exchange Coefficients

According to the previous study,[7] a percolation phenomenon was found for the diffusivities and surface exchange coefficients of mullite/zirconia composites. The diffusivities and surface exchange coefficients of low-zirconia composites were close to those of mullite, while the diffusivities and surface exchange coefficients of high-zirconia composites were close to those of zirconia. The characteristic lengths of low-zirconia composites were about 10^{-8}–10^{-6} m at 1000°–1350°C and those of high-zirconia composites were about 10^{-3}–10^{-2} m at 1000°–1350°C.

The mean particle size of any component in the porous sample was determined from quantitative image analysis:[20] $\bar{L} = 2V_V/S_V$ where V_V and S_V are the volume fraction of the component and the specific surface area of the porous sample, respectively. The mean particle size ($\bar{L}$) can be regarded as the thickness of the membrane ($2l$), i.e., the parameter l is equal to $\bar{L}/2$. The parameters l of all the composites were estimated to be about $2\text{–}4 \times 10^{-7}$ m in this study.

Generally speaking, the characteristic lengths of high-zirconia composites were much larger than their corresponding parameters l, and the relaxation processes in high-zirconia composites should be controlled by the surface exchange reaction. On the other hand, the characteristic lengths of low-zirconia composites approximated to their corresponding parameters l, and the relaxation processes in low-zirconia composites can be controlled by both surface exchange and diffusion processes.

Additionally, the flush time of the reactor volume (τ_f) can be given by[16]

$$\tau_f = \frac{V_r}{\Phi_V}\frac{T_{STP}}{T_r} \tag{10}$$

where Φ_V is the flow rate of gas, V_r and T_r are the reactor volume and absolute temperature, respectively, and T_{STP} is room temperature. In this study, the flow rate of gas was 1 L/min and the reactor volume was about 0.390 L. At 750°–1300°C, the flush time was estimated to be nearly 6.8–4.4 s, which was quite small and could be neglected with respect to the relaxation time of low-zirconia composites ($\approx 10^4$–10^2 s). However, the relaxation time of high-zirconia composites was close to the flush time. Therefore, the relaxation data of low-zirconia composites were fitted by Eq. (1) and those of high-zirconia composites were fitted by Eq. (7), whereby the oxygen diffusivities and surface exchange coefficients of various composites were obtained.

As listed in Table III, the oxygen diffusivities in low-zirconia composites ranged from 1.5 to 913 nm^2/s at 800°–1300°C. It was noted that the diffusivities in low-zirconia composites increased with increasing zircnoia content. The diffusivities calculated in this study were higher by 2–3 orders of magnitude than those measured by SIMS in the previous study.[7] The tracer diffusivities and chemical diffusivities were measured in the previous study and in this study, respectively. The chemical diffusivity (D_{chem}) and tracer diffusivity (D^*_{tr}) are correlated by the following expression:[21]

$$D_{chem} = D^*_{tr}(1 + (\mathrm{d}\ln\gamma_i/\mathrm{d}\ln C_i))$$

where γ_i and C_i are the activity coefficient and mole fraction of the species i, respectively. The term $(1+\mathrm{d}\ln\gamma_i/\mathrm{d}\ln C_i)$ is a thermodynamic factor and is considered as the difference between the chemical diffusivity and tracer diffusivity. Furthermore, the oxygen surface exchange coefficients of low-zirconia composites were in the range of 0.044–8.3 nm/s at 800°–1000°C. As listed in Table IV, the oxygen surface exchange coefficients of high-zirconia composites were in the range of 0.66–261 nm/s at 750°–850°C. This indicates that the surface exchange coefficients in low-zirconia composites increased with increasing zirconia content. However, those in high-zirconia composites (zirconia

Table III. Oxygen Diffusivities and Surface Exchange Coefficients of Low-Zirconia Composites at Various Temperatures and Oxygen Partial Pressures

	6.07→2.02 (kPa)	10.1→6.07 (kPa)	14.1→10.1 (kPa)	20.2→14.1 (kPa)
M				
1100°C				
D (nm^2/s)	1.7	1.5	3.6	3.9
α (nm/s)	0.078	0.077	0.044	0.045
1200°C				
D (nm^2/s)	27	23	29	16
α (nm/s)	0.39	0.52	0.23	0.56
1300°C				
D (nm^2/s)	86	110	103	88
α (nm/s)	1.6	4.2	1.9	1.7
MZY05				
1000°C				
D (nm^2/s)	3.5	4.7	4.4	7.9
α(nm/s)	0.15	0.10	0.16	0.20
1100°C				
D (nm^2/s)	43	24	35	40
α (nm/s)	0.33	0.17	0.37	0.45
1200°C				
D (nm^2/s)	62	90	72	101
α (nm/s)	0.99	0.87	1.2	1.5
MZY10				
900°C				
D (nm^2/s)	18	24	12	20
α (nm/s)	0.42	0.23	0.29	0.21
1000°C				
D (nm^2/s)	93	122	132	113
α (nm/s)	0.68	0.49	0.93	0.81
1100°C				
D (nm^2/s)	913	745	527	481
α (nm/s)	4.2	3.4	3.1	2.2
MZY20				
900°C				
D (nm^2/s)	20	40	26	50
α (nm/s)	0.43	0.89	0.55	0.84
1000°C				
D(nm^2/s)	116	278	272	258
α(nm/s)	3.6	2.6	2.0	1.9
1100°C				
D (nm^2/s)	594	586	696	888
α (nm/s)	6.8	7.5	11	5.4
MZY30				
800°C				
D (nm^2/s)	19	18	15	24
α (nm/s)	0.25	0.21	0.12	0.17
900°C				
D (nm^2/s)	97	43	55	60
α (nm/s)	0.96	0.39	0.46	0.34
1000°C				
D (nm^2/s)	358	566	241	410
α (nm/s)	8.3	3.9	1.7	2.3

content $\geq$50 vol%) were all similar. It was noted that oxygen surface exchange decreased with increasing oxygen partial pressure.

(3) Effects of Zirconia Content

From the Arrhenius plots of oxygen diffusivities and surface exchange coefficients, the corresponding activation energies can be estimated. Figure 5 shows the activation energies of oxygen diffusion and surface exchange versus zirconia content for various composites at various oxygen partial pressures. As shown in Fig. 5(a), the activation energies of oxygen diffusion decreased with increasing zirconia content and approached the results for low-zirconia composites measured in the previous study.[7] Figure 5(b) also illustrates that the activation energies of surface exchange decreased with increasing zirconia content, but the activation energies of surface exchange coefficients in high-zirconia composites approached that for zirconia.

Figure 6 shows the effect of zirconia content on the surface exchange coefficient in composites at 800°C. Note that the data for low-zirconia composites were obtained by extrapolation. There was a dramatic change in the surface exchange coefficient at about 40 vol% zirconia. This phenomenon can be explained by percolation theory[22,23] and effective medium theory.[24] Bruggeman's symmetrical effective medium theory[24] shows a percolation threshold at a conductor volume fraction of 0.33 in a three-dimensional case. The percolation threshold occurred at about 30–40 vol% zirconia, as shown in Fig. 6, which approximated the threshold value predicted by Bruggeman's symmetrical effective medium theory. It was noted that the surface exchange coefficient in mullite was much lower than those in low-zirocnia composites (MZY10–MZY30). This was attributed to the fact that the data for mullite were obtained via extrapolation, which has a greater uncertainty.

(4) Effect of Oxygen Partial Pressure

Figure 7 displays the relationship between the diffusivities and the oxygen partial pressures for various low-zirconia composites. There was no significant difference in the diffusivities of low-zirconia composites under various oxygen partial pressures. This could be explained by the fact that oxygen diffusion was correlated to the migration of oxygen vacancies, whose concentration was nearly constant in mullite or zirconia under the various oxygen partial pressures. It is noted that mullite is a nonstoichiometric compound and its chemical formula can be expressed as $Al_2[Al_{2+2x}Si_{2-2x}]O_{10-x}$, where x $(0.17 \leq x \leq 0.59)$ is the number of missing oxygen atoms per unit cell. The oxygen vacancies in mullite are formed due to the replacement of Si^{+4} ions by Al^{+3} ions, which can be expressed by the following equation:

$$Al_2O_3 \xrightarrow{SiO_2} 2Al'_{Si} + 3O_O^{\times} + V_O^{\bullet\bullet} \tag{11}$$

In addition, the formation of oxygen vacancies in Y_2O_3–ZrO_2 can be expressed by

$$Y_2O_3 \xrightarrow{ZrO_2} 2Y'_{Zr} + 3O_o^{\times} + V_O^{\bullet\bullet} \tag{12}$$

The concentrations of oxygen vacancies formed in mullite and zirconia are extrinsically fixed, and are independent of oxygen partial pressure in the range from 20.2 to 2.02 kPa. Therefore, the diffusivities of low-zirconia composites are independent of oxygen partial pressure.

Figure 8 illustrates the curves of the surface exchange coefficient versus the oxygen partial pressure for mullite at 1100°C, for low-zirconia composites at 1000°C and for high-zirconia composites at 800°C, respectively. The surface exchange coefficients of mullite, MZY20, MZY30, and high-zirconia composites (except MZY05 and MZY10) decreased with increasing oxygen partial pressure. In previous studies, a similar trend was reported between the surface exchange coefficient and oxygen partial pressure in yttria-doped ceria (YDC), yttria-stabilized zirconia (YSZ), or gadolinia-doped ceria (GDC).[25,26] Horita *et al.*[25] reported that there was a log–linear relationship between the surface exchange coefficient and oxygen partial pressure measured by SIMS in YDC and YSZ with a slope of about $-1/20$. Karthikeyan and Ramanathan[26] measured the surface exchange coefficient in thin-film GDC using the electrical conductivity relaxation method. They claimed that the limitation to the surface exchange rate of oxygen resulted from a reduction in

Table IV. Oxygen Surface Exchange Coefficients of High-Zirconia Composites at Various Temperatures and Oxygen Partial Pressures

	6.07→2.02 (kPa)	10.1→6.07 (kPa)	14.1→10.1 (kPa)	20.2→14.1 (kPa)
MZY40				
750°C α (nm/s)	0.80	0.76	0.66	0.67
800°C α (nm/s)	1.3	1.3	1.1	1.0
850°C α (nm/s)	2.0	1.8	1.8	1.7
MZY50				
750°C α (nm/s)	51	32	28	15
800°C α (nm/s)	137	71	46	36
850°C α (nm/s)	147	114	104	44
MZY60				
750°C α (nm/s)	48	33	30	24
800°C α (nm/s)	150	96	58	40
850°C α (nm/s)	160	108	85	65
MZY80				
750°C α (nm/s)	74	63	46	20
800°C α (nm/s)	181	102	69	37
850°C α (nm/s)	239	221	138	56
Z				
750°C α (nm/s)	94	79	64	66
800°C α (nm/s)	156	168	107	65
850°C α (nm/s)	261	217	196	212

the carrier concentration due to the segregation of Gd in near-surface regions.

(5) Rate-determining Mechanisms of Oxygen Surface Exchange

Horita *et al.*[25] reported that the rate-determining step for an oxygen surface exchange reaction in YDC and YSZ was the adsorption of oxygen at the gas/solid interface. However, Sirman and Kilner[27] indicated that the rate-limiting step for oxygen surface exchange might be the charge-transfer process in GDC and other fluorite materials. During the conductivity relaxation experiment, the surface exchange rate depended on the following reaction taking place at the gas/solid interface[28,29]:

$$\frac{1}{2}O_{2(g)} + 2e^- + V_O^{\bullet\bullet} \rightarrow O_O^{\times} \tag{13}$$

The reaction of Eq. (13) can be separated into several steps as follows:

$$\frac{1}{2}O_{2(g)} \rightarrow \frac{1}{2}O_{2(g,\,Pt\text{-pores})}\ (\text{gas-phase diffusion}) \tag{14}$$

$$\frac{1}{2}O_{2(g,\,Pt\text{-press})} + S_{ad} \rightarrow O_{ad}\ (\text{adsorption and dissociation}) \tag{15}$$

$$O_{ad} \rightarrow O_{ad(\text{reaction site})}\ (\text{surface diffusion}) \tag{16}$$

$$O_{ad}(\text{reaction site}) + 2e^- + V_O^{\bullet\bullet} \rightarrow O_O^{\times}\ (\text{charge-transfer reaction}) \tag{17}$$

The gas-phase diffusion coefficient within the O_2/Ar mixing gas can be calculated using the Chapman–Enskog equation:[30]

$$D_m = \frac{1.86 \times 10^{-3} T^{3/2} (1/M_1 + 1/M_2)^{1/2}}{p\sigma_{12}^2 \Omega} \tag{18}$$

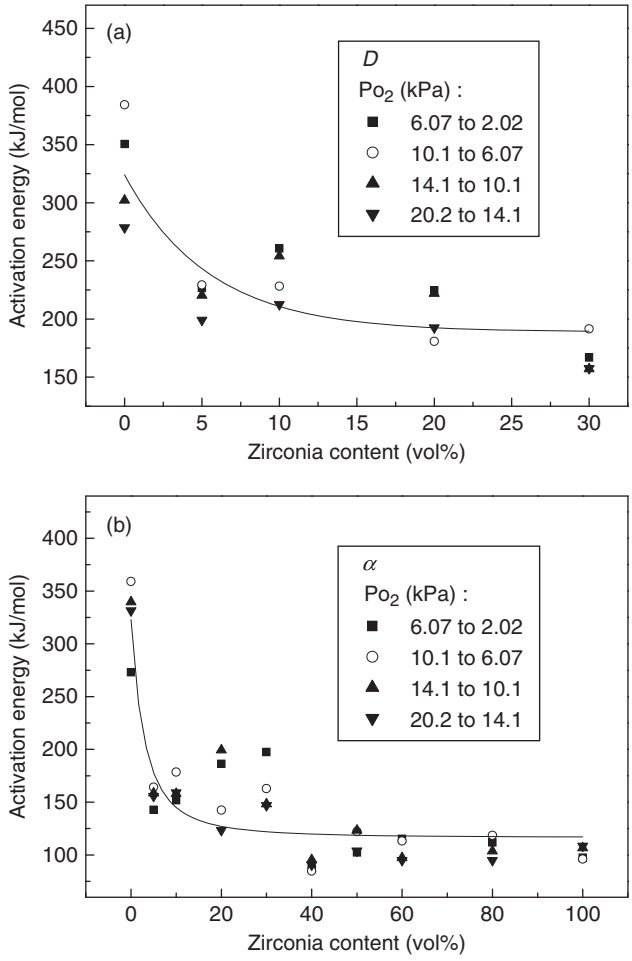

Fig. 5. The plot of the activation energy versus zirconia content in mullite/zirconia composites for (a) diffusion coefficients and (b) surface exchange coefficients.

where T is the temperature (K), M_1 and M_2 are the molecular weights of gas 1 and gas 2, p is the pressure (atm), σ_{12} is the collision diameter (Å), Ω is the nondimensional collision integral, and the unit of D_m is cm^2/s. When the mean free path of the gas is greater than the pore diameter, Knudsen diffusion should be considered. The Knudsen diffusion coefficient, D_{Kn}, is given by

$$D_{Kn} = 4850 d \sqrt{\frac{T}{M}} \tag{19}$$

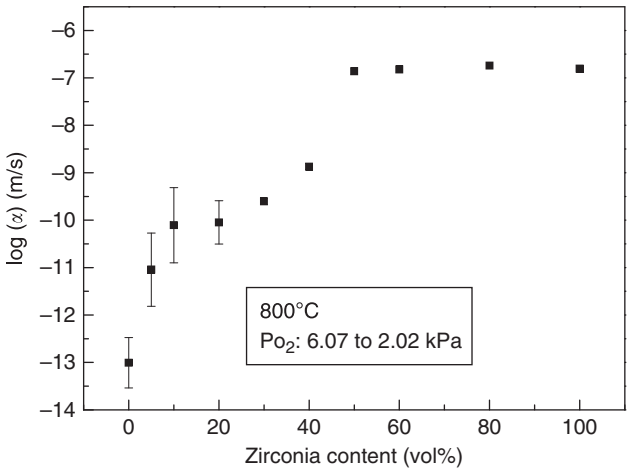

Fig. 6. Relationship between surface exchange coefficient and zirconia content at 800°C. The data of low-zirconia composites with error bars were obtained from the extrapolation.

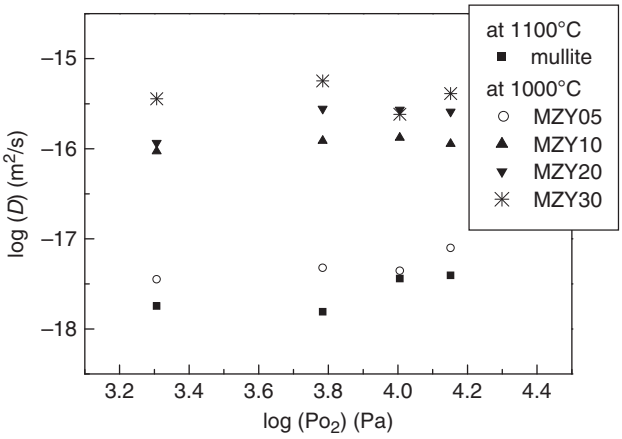

Fig. 7. Diffusivity versus oxygen partial pressure curves for monolithic mullite at 1100°C and low-zirconia composites at 1000°C.

where d is the pore diameter (cm), T is the temperature, M is the molecular weight, and the unit of D_{Kn} is cm^2/s. The effective diffusion coefficient, D_{eff}, of the gas through porous samples can be estimated by

$$D_{eff} = f_v \frac{D_p}{\tau} \tag{20}$$

where f_v is the void fraction, τ is the tortuosity (range between 2 and 6, averaging about 3), and D_p is the diffusion coefficient within the pores (i.e., D_m for mixing gas diffusion and D_{Kn} for Knudsen diffusion).

The calculated effective diffusion coefficients in the O_2–Ar mixing gas in this study were between 0.23 and 0.52 cm^2/s and those of Knudsen diffusion were between 0.25 and 0.55 cm^2/s. It was concluded that the effective diffusion coefficient for the mixing gas was very close to Knudsen diffusivities. However, they were much larger than the oxygen diffusion coefficients in those porous samples. Hence, gas-phase diffusion in porous samples could not be the rate-determining step (RDS).

In the previous studies[31,32] on the electrode reaction at the interface between Pt and yttria-doped zirconia, the RDS was the dissociative adsorption of oxygen on the Pt surface with an activation energy of about 154 kJ/mol for $T \leq 500$°C, while it was the surface diffusion of O_{ad} atoms on the Pt surface to the Pt/zirconia contact with an activation energy of about 171 kJ/mol for $T \geq 600$°C. Additionally, Yoon *et al.*[29] indicated that the RDS was the migration of oxygen vacancies to the triple phase boundary line at temperatures above 800°C and low oxygen pressures, based on the assumption that the charge-transfer reactions and adsorption and dissociation process are fast.

The equilibrium constant of Eq. (13) is expressed by the following equation:

$$K = [V_O^{\bullet\bullet}][e']^2 P_{O2}^{1/2} \tag{21}$$

When the concentration of oxygen vacancies in mullite (Eq. (11)) is higher than that of oxygen vacancies formed on the surface (Eq. (13)) (thermodynamical formation),[33] the relation to the defect concentration obtained from Eq. (11) can be described as follows:

$$[V_O^{\bullet\bullet}] = \frac{1}{2}[Al'_{Si}] \tag{22}$$

Combining Eq. (21) with Eq. (22) results in

$$[e'] = (2K)^{1/2}[Al'_{Si}]^{-1/2} P_{O2}^{-1/4} \tag{23}$$

Similarly, when the concentration of oxygen vacancies in zirconia is determined extrinsically by $[Y'_{Zr}]$, the relation to defect concentrations obtained from Eq. (12) can be described as follows:

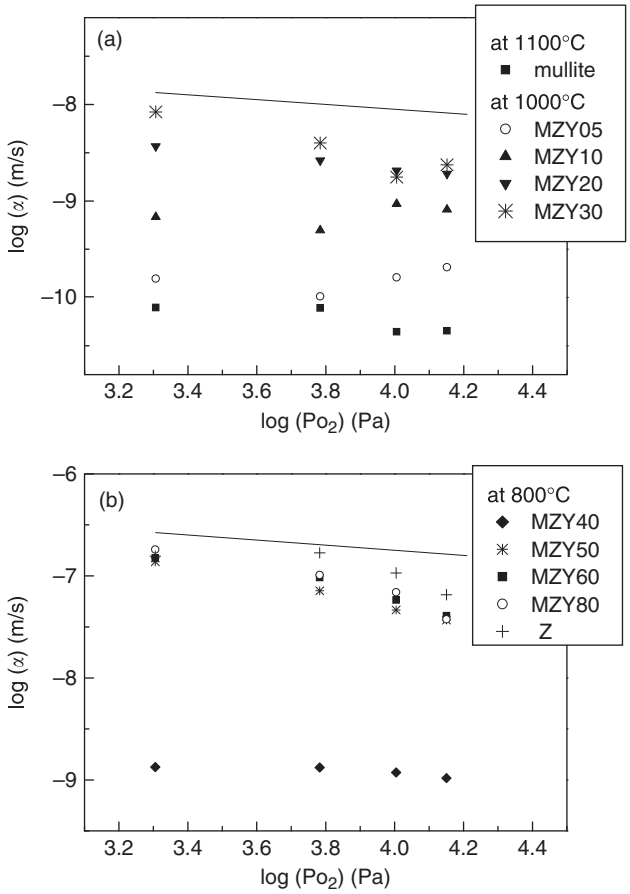

Fig. 8. Surface exchange coefficient versus oxygen partial pressure curves for (a) mullite at 1100°C and low-zirconia composites at 1000°C; (b) high-zirconia composites at 800°C. A slope of −1/4 is presented by the solid line.

$$[V_O^{\bullet\bullet}] = \frac{1}{2}[Y'_{Zr}] \tag{24}$$

Combining Eq. (21) with Eq. (24) results in

$$[e'] = (2K)^{1/2}[Y'_{Zr}]^{-1/2} P_{O2}^{-1/4} \tag{25}$$

The concentrations of electronic defects in mullite and zirconia are proportional to $pO_2^{-1/4}$. When the surface exchange coefficient is dominated by the charge-transport process, the slope of −1/4 for the logα–logpO_2 plot can be expected. Seeing that the slopes of the logα–logpO_2 plots for mullite/zirconia composites deviated slightly from −1/4, as shown in Fig. 8, it was inferred that the surface exchange rate was dependent on the concentration of electrons.

V. Conclusions

1. Oxygen diffusivities and surface exchange coefficients in porous low-zirconia composites can be measured using the conductivity relaxation method. However, the oxygen diffusivities in porous high-zirconia composites could not be determined because of the predominant surface exchange reaction.
2. The surface exchange coefficients in porous high-zirconia composites can be solely determined without considering diffusivities, because the surface exchange reaction was the rate-limiting step for porous high-zirconia composites.

3. Oxygen diffusivities and surface exchange coefficients in low-zirconia composites increased with the zirconia content, while the surface exchange coefficients in high-zirconia composites remained approximately constant.

4. The surface exchange coefficients in porous mullite/zirconia composites exhibited the percolation phenomenon with a threshold approximately at 40 vol% zirconia.

5. The oxygen diffusivities in porous low-zirconia composites were independent of the oxygen partial pressure at 2.02 kPa $\leq p\mathrm{O}_2 \leq$ 20.2 kPa. This implied that oxygen diffusion was related to the migration of oxygen vacancies because the concentration of vacancies was independent of the oxygen partial pressure.

6. The surface exchange coefficients in porous high-zirconia composites decreased with increasing oxygen partial pressure, with the slopes of the logα–log$p\mathrm{O}_2$ plots slightly deviating from $-1/4$. It was thus inferred that the surface exchange rate was dependent on the concentration of electrons.

References

[1]H. Schneider, K. Okada, and J. Pask, *Mullite and Mullite Ceramics*, pp. 1. John Wiley and Sons Ltd., New York, 1994.

[2]I. A. Aksay, D. M. Dabbs, and M. Sarikaya, "Mullite for Structural, Electronic, and Optical Applications," *J. Am. Ceram. Soc.*, **74** [10] 2343–58 (1991).

[3]N. Claussen and J. Jahn, "Mechanical Properties of Sintered, In Situ-Reacted Mullite-Zirconia Composites," *J. Am. Ceram. Soc.*, **63** [3–4] 228–9 (1980).

[4]Q. M. Yuan, J. Q. Tan, and Z. G. Jin, "Preparation and Properties of Zirconia-Toughened Mullite Ceramics," *J. Am. Ceram. Soc.*, **69** [3] 265–7 (1986).

[5]M. Ishitsuka, T. Sato, T. Endo, and M. Shimada, "Sintering and Mechanical Properties of Yttria-Doped Tetragonal ZrO_2 Polycrystal/Mullite Composites," *J. Am. Ceram. Soc.*, **70** [11] C342–6 (1987).

[6]R. Ruh, K. S. Mazdiyasni, and M. G. Mendiratta, "Mechanical and Microstructural Characterization of Mullite and Mullite-SiC-Whisker and ZrO_2-Toughened-Mullite-SiC-Whisker Composites," *J. Am. Ceram. Soc.*, **71** [6] 503–12 (1988).

[7]H. D. Ko and C. C. Lin, "Oxygen Diffusivities in Mullite/Zirconia Composites Measured by $^{18}O/^{16}O$ Isotope Exchange and Secondary Ion Mass Spectrometry," *J. Mater. Res.*, **23** [2] 353–8 (2008).

[8]H. D. Ko, C. C. Lin, and K. C. Chiu, "Effect of Zirconia Content on Electrical Conductivities of Mullite/Zirconia Composites Measured by Impedance Spectroscopy," *J. Mater. Res.*, **23** [8] 2125–32 (2008).

[9]J. J. Haslam and F. F. Lange, "Strengthening of Porous Mullite and Zirconia CMC Matrices by Evaporation/Condensation," *J. Am. Ceram. Soc.*, **89** [6] 2043–50 (2006).

[10]B. A. Latella and E. G. Mehrtens, "High Temperature Biaxial Strength of Porous Mullite-Alumina and Mullite-Zirconia Ceramics," *J. Mater. Sci.*, **42**, 5880–2 (2007).

[11]R. Ganeshananthan and A. V. Virkar, "Measurement of Surface Exchange Coefficient on Porous $La_{0.6}Sr_{0.4}CoO_{3-\delta}$Samples by Conductivity Relaxation," *J. Electrochem. Soc.*, **152** [8] A1620–8 (2005).

[12]S. Wang, A. Verma, Y. L. Yang, A. J. Jacobson, and B. Abeles, "The Effect of the Magnitude of the Oxygen Partial Pressure Change in Electrical Conductivity Relaxation Measurements: Oxygen Transport Kinetics in $La_{0.5}Sr_{0.5}CoO_{3-\delta}$," *Solid State Ion.*, **140** [1–2] 125–33 (2001).

[13]J. Crank, *The Mathematics of Diffusion*. 2nd edition, p. 60, Oxford University Press, New York, 1975.

[14]B. C. H. Steele, "Interfacial Reactions Associated with Ceramic Ion Transport Membranes," *Solid State Ion.*, **75**, 157–65 (1995).

[15]H. J. M. Bouwmeester and A. J. Burggraaf, "Dense ceramic membranes for oxygen separation"; pp. 481-553 in *The CRC Handbook of Solid State Electrochemistry*, Edited by P. J. Gellings, and H. J. M. Bouwmeester. CRC Press, Boca Raton, FL, 1997.

[16]M. W. den Otter, H. J. M. Bouwmeester, B. A. Boukamp, and H. Verweij, "Reactor Flush Time Correction in Relaxation Experiments," *J. Electrochem. Soc.*, **148** [2] J1–J6 (2001).

[17]A. Kopp, H. Nafe, and W. Weppner, "Characterization of the Electronic Charge Carriers in TZP," *Solid State Ion.*, **53–56**, 853–8 (1992).

[18]C. Schwandt and W. Weppner, "Electrode Reactions at Oxygen, Noble Metal/Stabilized Zirconia Interfaces," *Ionics*, **2**, 113–22 (1996).

[19]A. S. Patnaik and A. V. Virkar, "Transport Properties of Potassium-Doped $BaZrO_3$ in Oxygen- and Water-Vapor-Containing Atmospheres," *J. Electrochem. Soc.*, **153** [7] A1397–A405 (2006).

[20]H. E. Exner, "Stereology and 3D Microscopy: Useful Alternatives or Competitors in the Quantitative Analysis of Microstructures?," *Image Anal. Stereol.*, **23**, 73–82 (2004).

[21]H. Schmalzried, *Monographs in Modern Chemistry; Vol. 12: Solid State Reactions*, pp. 59. Verlag Chemie, Weinheim, 1981.

[22]S. Kirkpatrick, "Percolation and Conduction," *Rev. Mod. Phys.*, **45** [4] 574–88 (1973).

[23]V. K. S. Shante and S. Kirkpatrick, "An introduction to Percolation Theory," *Adv. Phys.*, **20** [85] 325–57 (1971).

[24]R. Landauer, "Electrical Conductivity in Inhomogeneous Media"; pp. 2–45 in *Electrical Transport and Optical Properties of Inhomogeneous Media*, Edited by J. C. Garland, and D. B. Tanner. American Institute of Physics Conference Proceedings, No. 40, New York, 1978.

[25]T. Horita, K. Yamaji, N. Sakai, M. Ishikawa, H. Yokokawa, T. Kawada, and M. Dokiya, "Oxygen Surface Exchange of $Y_{0.2}Ce_{0.8}O_{2-x}$ under Reducing Atmosphere," *Electrochem. Solid State Lett.*, **1** [1] 4–6 (1998).

[26]A. Karthikeyan and S. Ramanathan, "Oxygen Surface Exchange Studies in Thin Film Gd-Doped Ceria," *Appl. Phys. Lett.*, **92**, 243109 (2008).

[27]J. D. Sirman and J. A. Kilner, "Surface Exchange Properties of $Ce_{0.9}Gd_{0.1}O_{2-x}$ Coated with $La_{1-x}Sr_xFe_yCo_{1-y}O_{3-\delta}$," *J. Electrochem. Soc.*, **143** [10] L229–L31 (1996).

[28]O. J. Velle, T. Norby, and P. Kofstad, "The Electrode System O_2/Pt//ZrO_2: $8Y_2O_3$ Investigated by Impedance Spectroscopy," *Solid State Ion.*, **47**, 161–7 (1991).

[29]S. P. Yoon, S. W. Nam, S. G. Kim, S. A. Hong, and S. H. Hyun, "Characteristics of Cathodic Polarization at Pt/YSZ Interface without the Effect of Electrode Microstructure," *J. Power Sources*, **115**, 27–34 (2003).

[30]E. L. Cussler, *Diffusion: Mass Transfer in Fluid Systems*, 2nd edition p. 104, Cambridge University Press, Cambridge, UK, 1997.

[31]J. Mizusaki, K. Amano, S. Yamauchi, and K. Fueki, "Electrode Reaction at Pt, $O_{2(g)}$/Stabilized Zirconia Interfaces. Part I: Theoretical Consideration of Reaction Model," *Solid State Ion.*, **22**, 313–22 (1987).

[32]J. Mizusaki, K. Amano, S. Yamauchi, and K. Fueki, "Electrode Reaction at Pt, O_2(g)/Stabilized Zirconia Interfaces. Part II: Electrochemical Measurements and Analysis," *Solid State Ion.*, **22**, 323–30 (1987).

[33]Y. Hirata, M. Kawabata, and Y. Ishihara, "Electrical Properties of Silica-Alumina Ceramics in Nitrogen Atmosphere," *J. Mater. Res.*, **8** [5] 1116–21 (1993). □